ASTM Geotechnical Testing Journal. Submitted July 2018; Published February 2019.
https://doi.org/10.1520/GTJ20180204.

A CRS Oedometer Cell for Unsaturated and Non-Isothermal Tests

Meghdad Bagheri[1], Mohaddeseh Mousavi Nezhad[2], Mohammad Rezania[3]

[1]School of Energy, Construction and Environment, Coventry University, Coventry, UK

[2,3]School of Engineering, University of Warwick, Coventry, UK

Abstract

Research into the thermo-hydro-mechanical (THM) behavior of unsaturated soils and the effect of strain rate on their mechanical responses requires employment of advanced laboratory testing systems and procedures as well as protocols of correcting the measured data in order to account for errors associated with complex test conditions and apparatus calibrations. This paper presents design and calibration of an innovative constant-rate-of-strain (CRS) oedometer cell for characterization of the THM behavior of soils under combined non-isothermal and unsaturated conditions. The advanced oedometer cell enables for simultaneous control of temperature, suction, and stress state within the soil specimens. Temperatures of 20 to 200° C is applied through a tubular heating element placed at the base of the soil specimen. Suction is controlled using axis-translation technique, and measured using both axis-translation and two high-capacity tensiometers (HCTs) accommodated on the periphery of the specimen. The

[1] Email: ac6031@coventry.ac.uk
[2] Email: m.mousavi-nezhad@warwick.ac.uk
[3] Corresponding author, Email: m.rezania@warwick.ac.uk

ASTM Geotechnical Testing Journal. Submitted July 2018; Published February 2019.
https://doi.org/10.1520/GTJ20180204.

performance of the new cell is assessed based on a set of tests performed on clay specimens and its merits and advantages are discussed in detail.

Keywords: oedometer, strain rate, temperature, suction, tensiometer, water retention, calibration, compression tests.

List of Symbols

$\dot{\varepsilon_v}$ = volumetric strain rate
ΔL_T = thermally induced axial deformation
ΔT = temperature change
Δu = pore-water pressure change
ε_a = axial strain
σ_p = yield vertical net stress
σ_v = applied vertical total stress
c_v = coefficient of consolidation
G_s = specific gravity
I_p = plasticity index
s = soil suction
s_0 = initial suction
S_r = degree of saturation
T = temperature
u_a = pore-air pressure
u_{exc} = excess pore-water pressure
u_w = pore-water pressure
w = gravimetric water content
w_0 = initial gravimetric water content
w_L = liquid limit
w_P = plastic limit
AEV = air-entry value
CG = constant gradient
CL = continuous loading
CRL = constant rate of loading
CRS = constant rate of strain
D = grain size
HCT = high capacity tensiometer
IL = incremental loading
LC = London clay
LPT = linear potentiometric transducer
PSD = particle size distribution
PWPT = pore-water pressure transducer

ASTM Geotechnical Testing Journal. Submitted July 2018; Published February 2019.
https://doi.org/10.1520/GTJ20180204.

SWRC = soil water retention curve
TC = thermocouple
THM = thermo-hydro-mechanical

Introduction

Climate interacts with natural slopes and shallow depth soil deposits to cause changes in their hydro-mechanical properties mainly in terms of their pore-water pressure (u_w), strength and stiffness parameters (Delage et al. 2000; Burghignoli et al. 2000; Cekerevac and Laloui 2004). These deposits are typically encountered above the phreatic table and hence, are unsaturated. Under these conditions, different physical processes with high level of coupling take place. These processes mainly involve; (1) hydraulic processes such as liquid and/or vapor flow, stemming from groundwater recharge, precipitation, evaporation, and evapotranspiration (e.g. Ng and Xu 2012; Pagano et al. 2016), (2) thermal processes such as natural or artificial heat transfer induced by droughts, hot buried pipes and cables, and underground thermal energy storage systems (e.g. Salager et al. 2008; Uchaipichat and Khalili 2009), and (3) mechanical processes such as solid matrix deformations induced by sedimentation, progressive gravitational straining, and/or external loading (e.g. Lai et al. 2010; Zou et al. 2013). Moreover, it is well known that the mechanical behavior of soils, in particular natural soft soils, is highly influenced by time and rate effects (Bagheri et al. 2015; Rezania et al. 2016; Rezania et al. 2017). Experimental investigation and numerical modelling of soils behavior subjected to each of these processes are relatively complex and costly. The coupling of these processes can indeed further complicate the investigations, requiring advanced numerical modelling tools and laboratory and field testing equipment. The difficulty in control of several parameters in an experiment and to ensure their accurate measurement might be a reason for limited number of experimental studies on coupled effects of stress state, suction, and temperature (François and Laloui 2010). In all abovementioned processes, characterization of soils' one-dimensional (1D) stress–strain response is of high importance especially for serviceability and stability analysis

of geostructures. In the past few decades, researchers have been working on development of 1D testing equipment which allow for testing soils under controlled stress, strain, suction, and temperature conditions. Several apparatuses have been so far devised and constructed. A suction and temperature controlled oedometer cell was developed by Romero et al. (1995) at the Technical University of Catalonia (UPC), Spain. In this apparatus, axial stress is imposed through an air-pressurized stretchable diaphragm. Temperature is applied and regulated using a thermostatically controlled heater surrounding the cell, and suction is controlled using axis-translation technique which is based on measurement of air and water pressure differential across a high air-entry value (AEV) ceramic disk. A number of limitations associated with axis-translation method have been reported in the literature including; (1) the range of suctions that can be measured or applied is a function of the AEV of the ceramic filter as well as the maximum capacity of the pressurized air supply system, (2) lack of good contact between the pore-water and the water in the ceramic disk results in discontinuity of water flow through the porous filter and may dramatically increase the equilibrium time or even prohibit the drainage of water (Marinho et al. 2008), (3) accumulation of diffused air bubbles in high AEV ceramic can result in discontinuity between the specimen's pore-water and the water in the measurement system (Romero et al. 2003), (4) control of soil moisture evaporation can be rather difficult, requiring a careful setup of auxiliary devices such as vapor traps and diffused air flushing/volume indicator, especially when testing at high temperatures (Romero et al. 2003; Romero et al. 2005). Rampino et al. (1999) developed a suction controlled oedometer cell for unsaturated soils at Università di Napoli Federico II, Italy. Their design was based on the modifications applied to the device initially designed by Wissa and Heiberg (1969). This apparatus allows for running all types of continuous loading (CL) tests, i.e. CRS, constant rate of loading (CRL), and constant gradient (CG) tests. Axial stress in this system is applied directly through an air pressurized chamber connected to the loading cap of the cell. This

device, similar to the UPC oedometer, controls matric suction of the specimen using the axis-translation technique and, therefore, is prone to the drawbacks associated with this method. Tarantino and De Col (2008) performed static compaction tests on Kaolin Clay specimens inside an oedometer cell modified to measure suction variations using two HCTs accommodated on its loading cap. In this apparatus, the axial stress is applied to the sample using a pneumatic actuator, hence allowing for CRL tests to be carried out. CRS test results on undisturbed unsaturated Bapaume loess specimens using a modified oedometer cell were reported by Muñoz-Castelblanco et al. (2011). The oedometer cell is equipped with a HCT accommodated at the base of the specimen for direct measurement of soil suction evolutions during constant water content CRS tests carried out at rates of 0.003, 0.010, and 0.059 $\%min^{-1}$. Tarantino and De Col (2008) and Muñoz-Castelblanco et al. (2011) concluded that CRS tests are preferred over the conventional incremental loading (IL) tests for monitoring suction variations and that the IL tests are better adapted for saturated specimens. Design of a suction and temperature controlled oedometer cell at the Ecole Polytechnique Fédérale de Lausanne (EPFL), Switzerland, was also reported by François and Laloui (2010). In this device, the axial stress is applied through a water pressurized membrane made of a stretchable material. Heating is applied through circulating heated water in a ring-shaped chamber surrounding the specimen. Axis-translation is used as the suction control method. The drawbacks of this apparatus, however, can be outlined as; (1) use of stretchable membranes to transmit the vertical pressure to the specimen typically involves difficulties in calibration of membrane friction with the cell wall, (2) errors associated with membrane fatigue influences and modifies the mechanical loading transmitted to the specimen in long term use, and (3) the drawbacks of axis-translation technique, as explained above, can further influence the test results. A temperature controlled CRS oedometer cell was developed by Tsutsumi and Tanaka (2011) at Hokkaido University, Japan. A high accuracy stepper motor system is utilized in this apparatus for loading the

specimen under very small strain rates. An external load cell placed at the bottom of the cell is used to measure the axial stresses. The specimen's temperature is controlled through circulation of an isothermal liquid inside a metal pipe spiraled around the specimen. A thermocouple attached to the upper platen of the consolidation cell is used for measurement of temperature variations. The main drawback of this device is the use of external load cell which involves errors associated with the friction between the loading ram and the guide shaft. Coccia and McCartney (2016) studied the thermal volume change of unsaturated compacted Bonny silt in a high pressure thermal isotropic cell equipped with pressure-volume controllers to track changes in degree of saturation. In this cell, matric suction is controlled via the axis translation technique. The thermal volume change behavior of soils with different stress histories was found to be significantly influenced by the secondary compression response. Most recently, a temperature controlled CRS oedometer cell was developed by Jarad et al. (2017) at Université de Lorraine, France. This cell is installed in a load frame capable of running strain-controlled tests in range of 0.002 – 0.02 $\%min^{-1}$. A temperature range of 5 to 70º C could be applied to the specimen through circulation of a thermal liquid in a spiral tube positioned around the cell (similar to the cell developed at Hokkaido University). The cell chamber is filled with water to ensure fully saturated conditions throughout the experiments. Ng et al. (2017) developed a thermal oedometer with invar ring and studied the effect of boundary conditions on cyclic thermal strains of clay and sand samples. In this cell, cyclic heating and cooling is applied through heat exchange with the heated water circulated through a spiral tube placed around the soil specimen.

The advanced apparatuses discussed above generally suffer from technical design drawbacks that restrict their application for long-term tests and over a wide range of soil suction and temperatures. For example, using axis-translation method to control matric suction in a specimen subjected to a long-term 1D creep or stress relaxation test can cause excessive

evaporation of soil water as well as air diffusion through the ceramic disk and hence, errors in monitoring suction and volume change evolutions. This paper presents the design and calibration of a new oedometer cell for conducting strain controlled compression tests while controlling and measuring suction and temperature of the specimen. Incorporation of two suction control and measurement methods, i.e. axis-translation and HCT, allows for successful monitoring of soil matric suction during short-term and long-term consolidation and stress relaxation tests with minimal errors. Conducting 1D compression tests under controlled strain rate, suction, and temperature requires rigorous calibrations and experimental techniques. The experimental procedures for correcting the applied conditions and measured data during experiments are discussed in details and some preliminary test results highlighting the coupled effects of strain rate ($\dot{\varepsilon}_v$), soil suction (s), and temperature (T) on compressibility of clay samples are presented.

The New CRS Oedometer

CELL LAYOUT

Fig. 1 shows a schematic diagram of the cell structure. The outer cell body is made of AISI 304 stainless steel whereas the inner cell and the confining ring are made of brass. The cell wall is designed to be thick enough to support the specimen and prevent lateral deformation, and hence satisfy the k_0 conditions. To minimize the disturbance to the specimen, the loading cap is made of a lightweight material i.e. aluminium. Cylindrical soil specimens of 95 mm diameter and 35 mm height can be tested in this apparatus. These dimensions are compatible with the minimum specimen diameter to thickness ratio of 2.5 recommended by ASTM D4186-06, *Standard Test Method for One-dimensional Consolidation Properties of Saturated Cohesive Soils Using Controlled-strain Loading*. Generally, the in-situ settlement rates of full-scale structures are much greater than those obtained from conventional oedometer tests on small size specimens

(e.g. 75 mm diameter × 20 mm thickness). This can be attributed to the effect of the clay macrofabric on drainage behavior (Rowe and Barden 1966). In fact, the macrostructural properties of clay layers such as presence of thin layers of silt and sand, organic inclusions, and silt-filled fissures can increase the overall permeability of the clay deposit and hence, increase settlement rates (Craig 2004). Garga (1988) performed oedometer tests on fissured London Clay (LC) specimens of various diameters and reported that the coefficient of consolidation (c_v) from 100 mm dimeter specimens were approximately 50% higher than 76 mm diameter specimens. More recently, Gasparre (2005) reported that the existence of fissures in 100 mm diameter specimens of intact LC can be the most possible reason for the observed differences in shear strength of 100 mm and 38 mm diameter specimens in triaxial tests. Therefore, in order to obtain more realistic predictions of soil settlements in laboratory, it is necessary to perform experiments on specimens large enough to represent structural (macrofabric) features of natural clays. In the new CRS cell, an increase in the diameter and the height of the specimen by respectively 27% and 75%, resulted in an increase in the specimen's volume by 181%, increasing the possibility of capturing macrostructural effects on hydro-mechanical properties. Furthermore, the selected dimensions allows for coring undisturbed specimens from U100 tube samplers with minimum disturbance.

ASTM Geotechnical Testing Journal. Submitted July 2018; Published February 2019.
https://doi.org/10.1520/GTJ20180204.

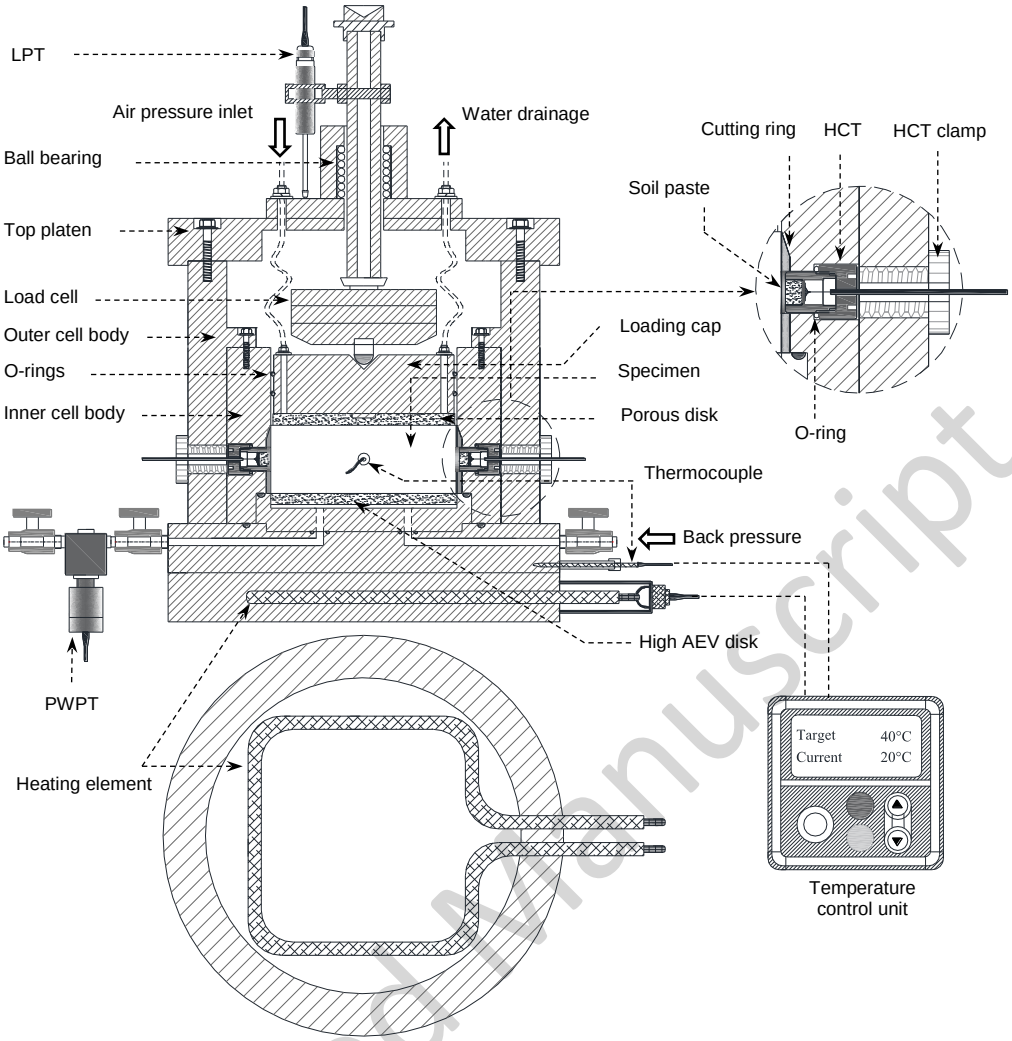

163

164 Fig. 1 Schematic diagram of the CRS cell structure and components

165 *STRESS/STRAIN CONTROL AND MEASUREMENT*

166 The apparatus is a load frame based system (Fig. 2) where the loading is generally via feedback
167 from a velocity controlled load frame. The loading frame has a maximum compressive strength
168 of 50 kN and speed range of 10^{-5} – 10 mm/min for constant rate of displacement. A 25 mm
169 travel length linear potentiometric transducer (LPT) placed on the top platen of the cell
170 provides measurement of axial strain and, therefore, volume change of the specimen. Axial
171 force is measured by an internal 25 kN submersible load cell guided through a ball bearing
172 shaft on the top platen of the cell. The use of internal load cells rectifies the adverse effect of
173 friction on measurements typical of conventional external load cells. This improvement is

highlighted during creep and stress relaxation tests (Fodil et al. 1997). The load cell is screwed to the loading cap and, from the other end, to the load frame to allow for strain controlled unloading of the specimen.

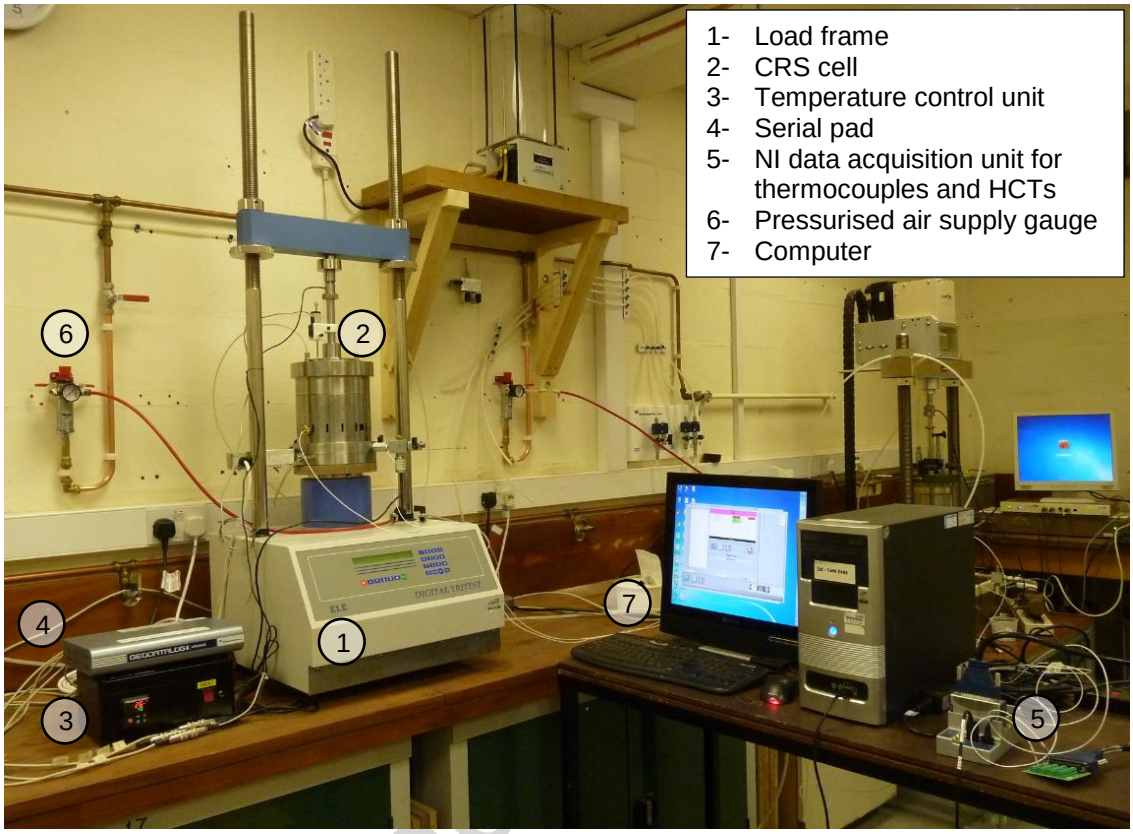

Fig. 2 The CRS system layout

MATRIC SUCTION CONTROL AND MEASUREMENT

The specific design of the CRS oedometer cell enables performance of strain controlled consolidation tests under both saturated (pore-water pressure control) and unsaturated (suction control) conditions. A 1.5 MPa high AEV porous disk placed at the bottom of the specimen allows for testing soil specimens under suction controlled conditions. Matric suctions of up to 1.0 MPa can be imposed using axis-translation technique. Pore-air pressure (u_a), supplied from a high-pressure air compressor and regulated by a pressure panel, is applied to the top of the specimen. The porous stone at the top of the specimen helps for uniform distribution of air pressure across the sample area. Pore-water pressure (u_w) is controlled at the bottom of the

specimen and regulated by an air-water interface (bladder) and a pressure panel. Using axis-translation technique for applying suction to the specimen typically involves evaporation of soil water, and the generation of vapor fluxes causes unwanted variation of suction inside the specimen. This effect is further highlighted when testing unsaturated specimens under high temperatures. To restrict the vapor transfer, as suggested by François and Laloui (2010), a vapor trap was installed in the air pressure line to humidify the pressurized air and maintain a high order of relative humidity throughout the experiments. Moreover, as recommended by Romero et al. (2005), to control the air diffusion across the high AEV ceramic disk, a flushing system was incorporated at the base of the cell, to periodically flush the diffused air bubbles. The spiral circuit machined inside the pedestal and underneath the porous disk further helps in collection of the diffused air bubbles from the system (Rampino et al. 1999). A 3.5 MPa pore-water pressure transducer (PWPT) is used for measurement of positive u_w at the base of the specimen. Water volume exchanges are measured using a semi-automatic volume change apparatus looped with the bladder and the pressure panel. Furthermore, two in-house made HCTs (see Bagheri at al. 2018) accommodated over the periphery and at the mid height of the specimen provide continuous measurement of matric suction during the experiments. Accommodating HCTs over the periphery and at the mid-height of the specimen allows for measurement of an average u_w during the tests. HCTs can be also used for local measurement of positive u_w inside the specimen. The specific assembly of the tensiometers inserts enables for replacement of cavitated tensiometers during the experiments without any interruption to the tests and disturbing the specimen.

TEMPERATURE CONTROL SYSTEM

The heating system consists of a WATROD double-ended tubular heater element (supplied by Watlow Ltd), placed at the base of the cell, and two J-type thermocouples for measurement and monitoring of temperature variations on the cell's body and inside the specimen. A temperature

control unit is used for setting target temperatures and monitoring feedbacks from the thermocouples. Temperature variations inside the specimen are measured by a thermocouple (TC1) placed close to the specimen. Another thermocouple (TC2) located close to the heater records the cell temperature. The signal feedback from this thermocouple is used to keep the temperature constant by acting on the thermostat in the control unit. The heating system enables testing soil specimens over a temperature range of 20 to 200° C. The average heating/cooling rate is approximately 3º C per minute on automatic mode. This rate can also be manually controlled by setting target temperatures at pre-defined time intervals. For example, a temperature change of 30º C could be ramped up over 30 minutes if the unit is set to increase the temperature for 1º C at every minute. An isolating ring made of Tufnol material is placed between the cell base and the loading piston's platen to prevent any possible damages to the stepper motor as a result of heat transfer.

DATA ACQUISITION

An 8 channel serial pad (GEODATALOG8 supplied from Controls Testing Equipment) was used for data acquisition from the transducers (load cell, LPT, and PWPT). The built-in data acquisition software enables for offline monitoring and storage of the data. The HCTs measurements were also monitored using a National Instruments (NI) data acquisition system and LabVIEW software. A LabVIEW code was also developed for monitoring the feedback data from the thermocouples. All the feedback data from the transducers and the temperature control unit were continually stored on a computer.

Calibration Procedures

As for any laboratory testing systems, a rigorous calibration was necessary in order to account for the errors associated with temperature change and mechanical adjustments during experiments. To this end, an assessment of (i) the effect of friction between the loading cap's

O-ring and the internal wall of the cell, (ii) the expansion and contraction of the cell under temperature changes, (iii) the effect of temperature on HCTs, and (iv) the thermal equilibrium between the heating system and the specimen were carried out and necessary calibrations were applied. In the following subsections, the results of these calibrations are presented.

INNER WALL FRICTION

Friction between the loading cap's O-rings and the internal wall of the cell as well as between the sample and the inner wall of the cutting ring, are the main sources of possible sidewall friction. In order to minimize the effect of sidewall friction on the measured forces several methodologies can be considered. Lubricating the O-rings on the loading cap as well as the internal cell body and the inner periphery of the cutting ring, with a very thin layer of grease, can to some extent reduce the sidewall friction (Seah and Juirnarongrit 2003). Attention must be applied not to leave high amount of grease on the cutting ring's inner wall, as grease can influence the inter-particles friction within the soil specimen and modify the consolidation process. François and Laloui (2010) performed a set of mechanical loading and unloading on water placed in the sample chamber in order to quantify the effect of friction between the loading membrane and the cell wall. A linear relationship was observed between the applied and measured pressures showing 5 – 6% difference. Sample-Lord and Shakelford (2012) performed a set of CRS consolidation tests on soil slurries containing bentonite and granular zero valent iron in acrylic columns and reported that the increase in strain rate will increase the induced friction between the top platen O-rings and the inner walls of the test cells. In this study, the inner wall of the internal cell was polished to produce a very smooth and glossy surface. Moreover, the loading cap's O-rings, the inner cell wall and the inner wall of the cutting ring were lubricated with a very thin layer of Vaseline to further minimize any potential side friction effect. Given the use of internal load cell in this work to allow for direct

measurement of the applied load at the contact point at the top of the specimen, calibration to account for the side friction was not carried out in this study.

CELL DEFORMATION UNDER CHANGES IN TEMPERATURE

The deformability of the cell structure under temperature changes can be investigated in the aspects of (i) the thermal expansion of the cell which can modify the measurements of the axial strains, and (ii) the thermal expansion of the cutting ring which can alter the oedometric conditions by posing undesirable radial deformations. Some researchers including Romero et al. (2003) and François and Laloui (2010) investigated the thermal expansion effects on the oedometric conditions and expressed that thermal strain of the soil particles partially offsets the thermal expansion or contraction of the cutting ring and, therefore, the oedometric condition is not significantly affected during non-isothermal experiments. Hence, it is only the thermal effect on the axial strains that needs to be taken into account when correcting the obtained test data. To this end, a simple calibration procedure was carried out. A cylindrical AISI 304 stainless steel sample with known coefficient of thermal expansion was placed inside the cell. Afterwards, the cell was subjected to a heating and cooling cycle of 25 to 75° C in steps of 10° C, and the corresponding axial deformation due to the thermal expansion of the sample and metallic cell body was measured by the LPT. Having known the thermal dilation of the stainless steel sample, the induced thermal dilation of the cell structure was deduced. Fig. 3 presents the measured and corrected thermally induced deformation of the cell structure. The observed differences in measured vertical displacements associated with heating and cooling cycles might be due to the insufficient time given during cooling steps for thermal equilibrium and recovery of thermally induced elastic strains. The axial deformation due to the effect of temperature (ΔL_T) appears to vary linearly with applied temperature change (ΔT) and can be approximated using the following linear correlation;

ASTM Geotechnical Testing Journal. Submitted July 2018; Published February 2019.
https://doi.org/10.1520/GTJ20180204.

$$\Delta L_T = -0.0029 \Delta T \quad (1)$$

The fact that the obtained values of ΔL_T are negative indicates that the thermal dilation of the cell structure results in a compressive deformation. Basically, during compression, the axial downward movement of the loading ram implies negative displacement measurement by the attached LPT (its shaft moves upward). Similarly, thermal expansion of the cell and top platen results in upward movement of the LPT's shaft, given that the loading ram is fixed to the load frame. It must be mentioned that the thermal expansion of the frame is disregarded, as the isolating ring made of Tufnol material, placed between the cell base and the loading piston's platen, prevents any possible heat transfer to the load frame. Moreover, a temperature range of 20 to 80º C has been considered in most published works on the effect of temperature on THM properties of clayey soils (e.g. Delage et al. 2000; Burghignoli et al. 2000; Cekerevac and Laloui 2004; François and Laloui 2010; Jarad et al. 2017). Therefore, the same range was considered in this work for calibrating the presented CRS cell and carrying out the preliminary experiments. It must be mentioned here that same calibrations may not be extrapolated for higher temperatures. Indeed, calibration and experimental investigations over the higher temperatures (>75º C) will be the subject of future studies using this apparatus.

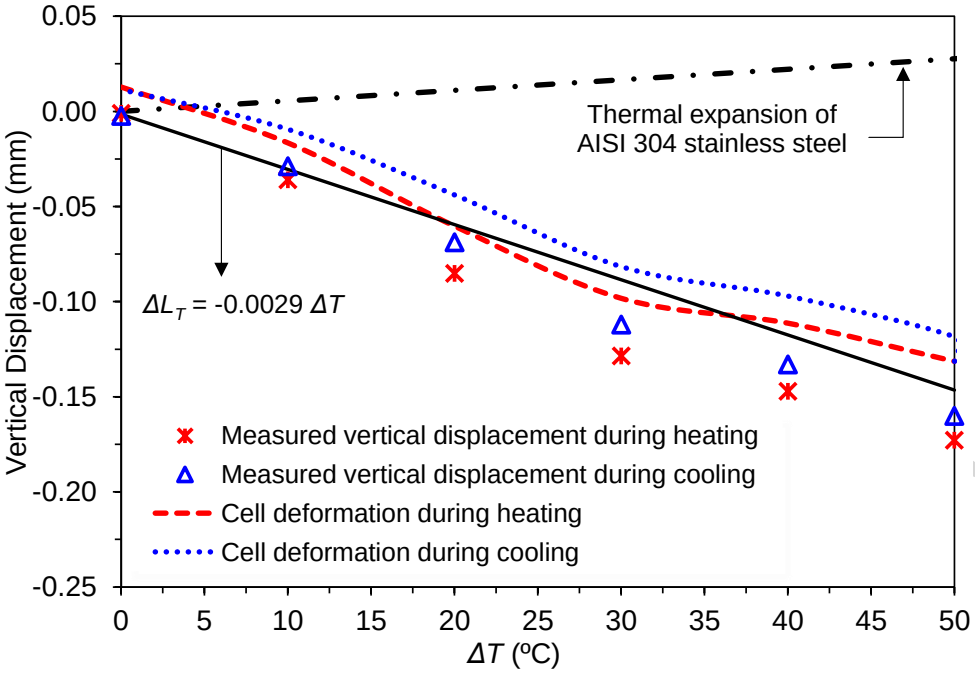

Fig. 3 Effect of thermal expansion of the cell on the measured axial deformations

EFFECT OF TEMPERATURE ON HCT

The HCTs were saturated and calibrated in an in-house made stainless steel saturation chamber (Fig. 4) following the procedure described in Bagheri et al. (2018). The saturation chamber possesses 8 slots to insert and clamp the HCTs in a way that their ceramic filter is faced inward and prone to de-aired de-mineralized water. A screw piston positioned at the centre of the chamber enables pressurization of the fluid inside the chamber. In order to evaluate the effect of temperature on HCT calibrations, the HCTs were subjected to a loading and unloading cycle inside the chamber, at two different temperatures of 25 and 60º C (Fig. 5). The obtained curves exhibited a linear trend both for loading and unloading cycles. A linear extrapolation to the calibration equation was developed for the pressures in negative range. An increase in temperature resulted in an increase of voltage output and shift of the calibration curve, yet the calibration coefficient was not affected notably. Considering the linear dilation of the HCT's AISI 304 stainless steel body (see Fig. 3), it was assumed that the shift in voltage output with temperature is also linear, resulting in an increase of the voltage output by 1 μV per 1º C increase of temperature, corresponding to an increase in suction measurements by

ASTM Geotechnical Testing Journal. Submitted July 2018; Published February 2019.
https://doi.org/10.1520/GTJ20180204.

318 approximately 10 kPa. Similar results were obtained for the other HCTs used. The data
319 obtained from HCTs during non-isothermal tests (see next section) were, therefore, adjusted
320 for the differences in calibration constants obtained during calibration of the HCTs at
321 corresponding temperatures.

ASTM Geotechnical Testing Journal. Submitted July 2018; Published February 2019.
https://doi.org/10.1520/GTJ20180204.

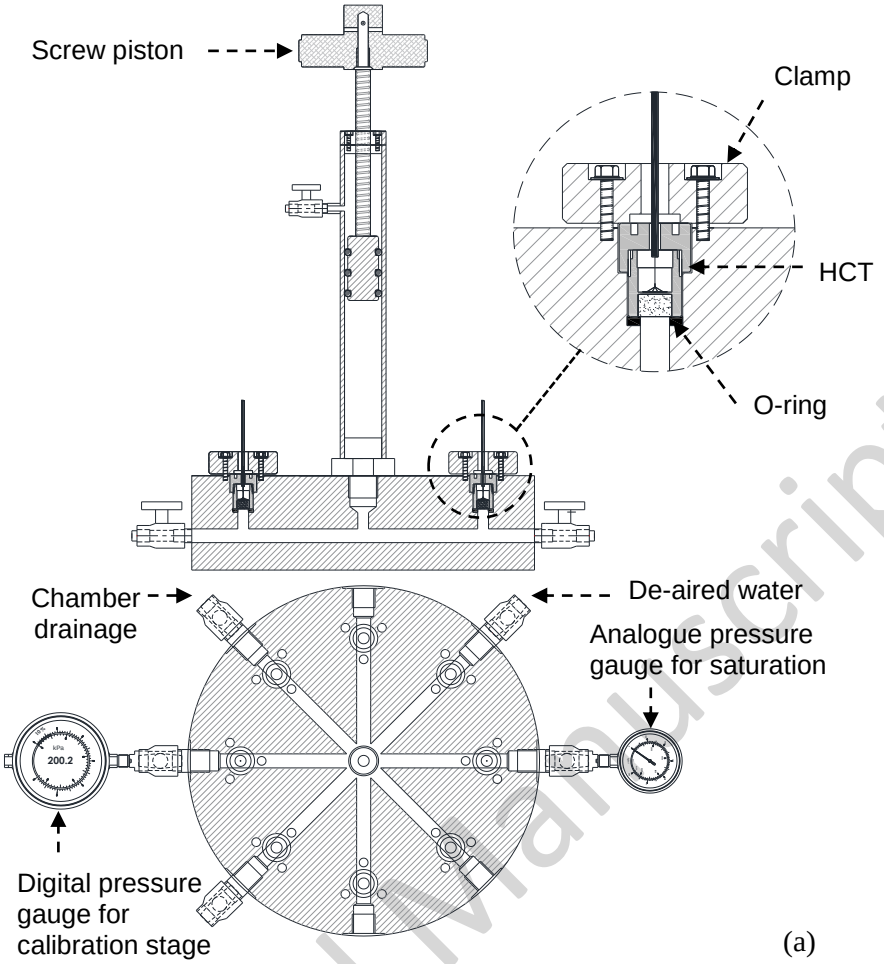

322 Fig. 4 Saturation chamber: (a) schematic diagram; (b) photo

ASTM Geotechnical Testing Journal. Submitted July 2018; Published February 2019.
https://doi.org/10.1520/GTJ20180204.

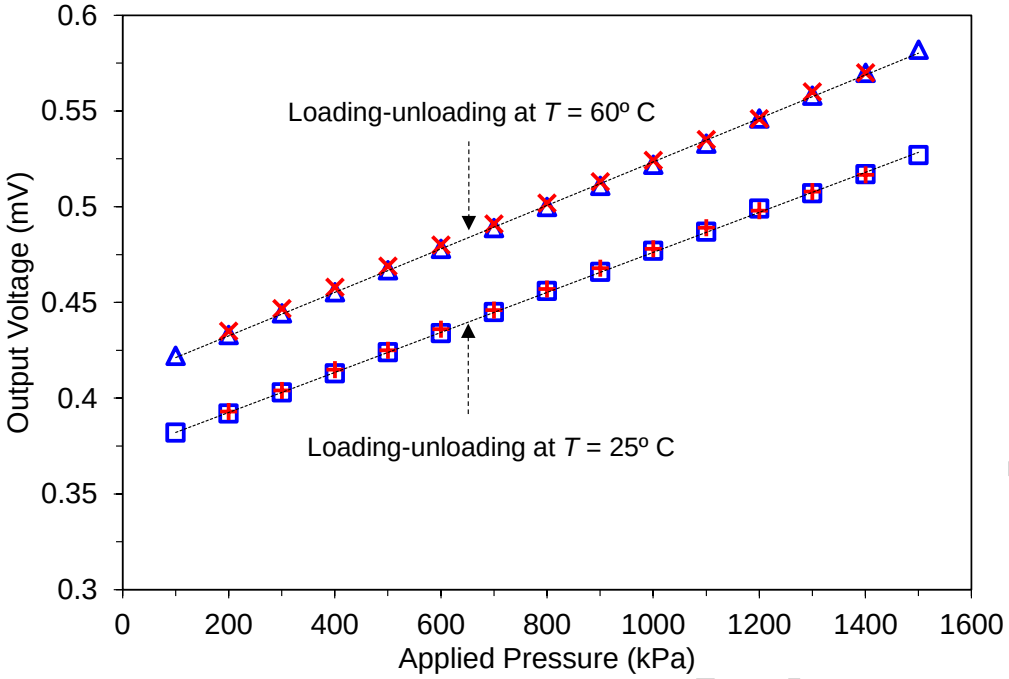

Fig. 5 Effect of temperature on HCT calibration

TEMPERATURE EQUILIBRIUM

Due to the difference in thermal conductivity of the cell body and the soil specimen, a delay in thermal equilibrium between the heating system and the soil specimen was expected. In order to quantify this time lag, the cell was subjected to a thermal cycle of 25 to 65°C in steps of 10°C. Temperature variations during each step were recorded for approximately 50 minutes. The thermal variations inside the saturated soil specimen was monitored using the thermocouple TC1, while the thermal variations of the heating system was monitored using the thermocouple TC2. It was observed that thermal equilibrium for each step of heating or cooling was obtained in approximately 40 minutes (Fig. 6). The temperature control unit enables applying a constant target temperature over the course of experiments, hence, maintaining thermal equilibrium between the heating system and the soil specimen. At equilibrium, there were not significant differences between the temperature in the heating system and the soil specimen, indicating the efficiency of the isolating system. The significant reduction in the equilibrium time in comparison with the similar temperature controlled systems presented in

339 the literature (e.g. François and Laloui 2010) is believed to be due to the heating from the base
340 of the specimen which rectifies, to some extent, the delays associated with thermal conductivity
341 of the metalic cell body. Moreover, direct heating of the cell's stainless steel base, using the
342 element heater, accelerates the thermal diffusion process in the metalic cell base. Therefore,
343 the thermal diffusion process in the soil mass may have more contribution to the observed
344 thermal equilibrium delay than the thermal diffusion in cell body.

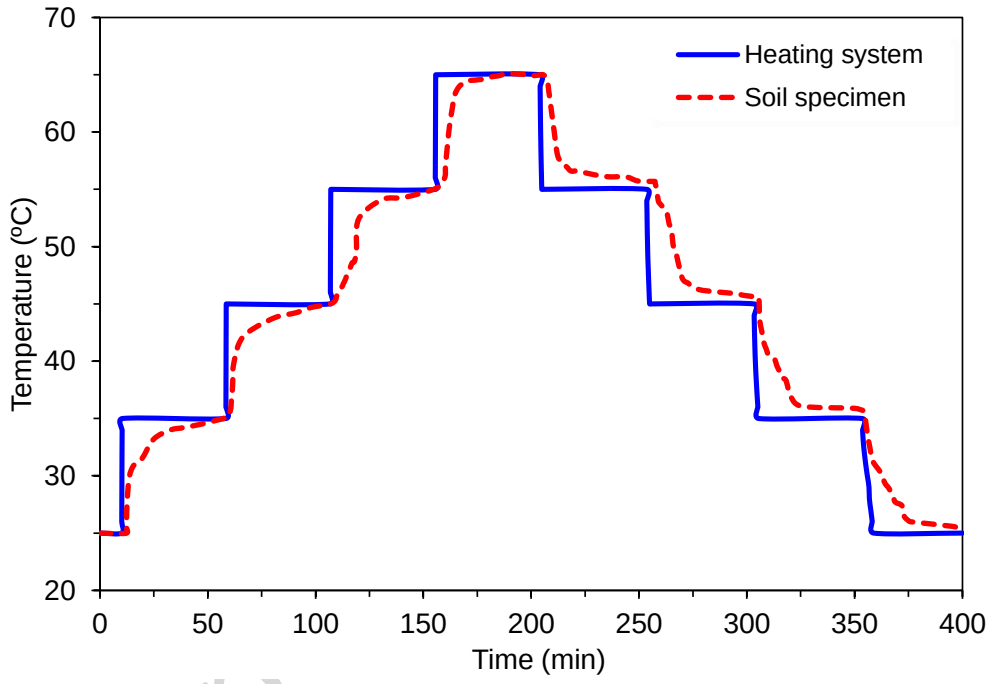

345

346 Fig. 6 Time lag in temperature equilibrium between the heating system and the soil specimen

347 Preliminary Tests

348 *MATERIAL AND SPECIMEN PREPARATION*

349 The material used for these tests was LC which was collected from an engineering site in Isle
350 of Sheppey, UK. To avoid complications associated with microfabric of undisturbed and
351 compacted soils, reconstituted samples were used for this set of experiments. The samples were
352 oven dried for 48 hours, then crushed into powder, and sieved through a 1.18 mm sieve.
353 Reconstituted soil samples were prepared by mixing the soil powder with distilled water at
354 initial water content of $w_0 = 1.5w_L$ until a homogenous paste was obtained. The paste was then

consolidated in a 120 mm diameter Perspex consolidometer under a vertical stress of 80 kPa for a duration of 5 days. The sample was then quickly unloaded to avoid any swelling and water absorption. The obtained cylindrical sample was then cut into three equal pieces and allowed to dry at room temperature to pre-specified water contents. Each sub-sample was placed on a course porous stone and inside a perforated chamber for relatively uniform water evaporation. The porous stone was used to facilitate the dynamic drying process by exposing the specimen's base to atmosphere. The unsaturated samples were then stored in air-tight containers for 24 hours for moisture equilibrium. Finally, the test specimens were prepared by carefully penetrating the oedometer ring into the samples and trimming off the excess soil. It must be noted that presence of course-grained peds (or large size clay clusters according to Le et al. 2012) resulted in an AEV value of around 260 kPa which is notably lower than the AEV of natural LC reported in the literature. The lower AEV made it possible to test specimens over a wider range of suctions, lying on the desaturation phase of the soil water retention curve (SWRC). Table 1 summarizes the index and physical properties of the reconstituted soil samples.

Table 1. Index and physical properties of the reconstituted LC samples

Grain size, D (mm)			Index properties			
D < 0.002	0.002 < D < 0.063	D > 0.063	w_P	w_L	I_P	G_s
58%	30%	12%	18%	68%	50%	2.67

EXPERIMENTAL PROCEDURE

Before commencing each experiment, the preparation of the cell was carried out. The drainage lines and the pressure transducer block were de-aired by means of vacuum and filled with de-aired water. The lower and upper porous discs were also saturated. Functionality of all transducers were checked and the load cell, LPT, and PWPT were zeroed. The specimen was then placed inside the cell chamber. The two HCTs, which were preconditioned according to

the procedure described by Bagheri et al. (2018), were then installed on the periphery of the specimen and gently clamped. Ultimate contact between the HCTs and the specimen was ensured by applying soil paste to the HCTs' porous disks. The loading cap, with its lubricated O-rings, was then positioned on top of the specimen and the load cell together with the top platen were placed and fastened. The cell was set up on the load frame and an initial vertical stress of 10 kPa was applied to the specimen to eliminate any possible bedding effects. The HCTs were allowed to equilibrate for 2 – 3 hours. Axial load was applied to the specimen from the piston moving upwards at constant rate of displacement, compressing the specimen inside the confining ring. Drained CRS compression tests with continuous pore-water pressure (suction) monitoring were carried out on reconstituted specimens at two different initial water contents of 32 and 33%, and two different temperatures of 22 and 50º C. Two different strain rates of 4.8×10^{-7} (denoted by letter A) and 2.4×10^{-6} s^{-1} (denoted by letter B) were selected and used for this set of experiments. The values of strain rates were selected so as to be; (1) compatible with the practical range of strain rate suggested by Pereira and De Gennaro (2010), and (2) fast enough to prevent development of structuration and resistance against loading with time. The selected strain rates were both too fast to allow fully drained conditions. Excess pore-water pressure (u_{exc}) was, therefore, built up during the loading stage. Tests were performed in temperature controlled laboratory environment to avoid the influence of temperature fluctuations on the output data. In addition to the compression behavior, the water retention behavior of the test material was also investigated. Table 2 summarizes the details of the CRS tests. Fig. 7 shows the generalized THM paths followed in the experimental program in a three-dimensional stress-suction-temperature space.

ASTM Geotechnical Testing Journal. Submitted July 2018; Published February 2019.
https://doi.org/10.1520/GTJ20180204.

Table 2. Details of the CRS tests

Test No.	w_0 [%]	s_0 [kPa]	T [ºC]	$\dot{\varepsilon}_v$ [s^{-1}]	σ_p [kPa]
CRSru33-A	33	701	22	4.8×10^{-7}	390
CRSru33-A50	33	701	50	4.8×10^{-7}	295
CRSru33-B	33	701	22	2.4×10^{-6}	480
CRSru32-A	32	802	22	4.8×10^{-7}	490

r: reconstituted, u: unsaturated, A and B: strain rates
The number before dash indicates initial water content.

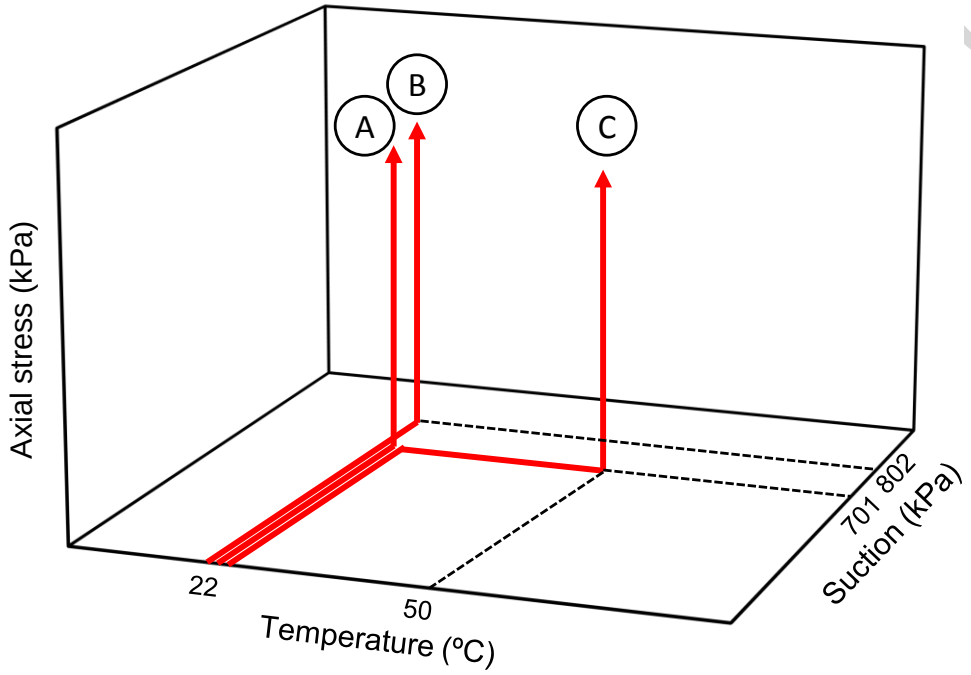

Fig. 7 Generalized THM paths followed in the experimental program. Paths A and B: isothermal compression with suction and strain rate control (CRSru33-A, CRSru33-B, and CRSru32-A); Path C: non-isothermal compression with suction and strain rate control (CRSru33-A50)

TEST RESULTS

Fig. 8 presents the obtained SWRC (gravimetric water content versus soil suction). The water retention characteristics of the soil specimen was measured in the new oedometer cell using axis-translation technique. Moreover, in order to develop a comparison platform, the water retention curve of an identical specimen was also measured in the new oedometer cell using the HCTs. Lower water contents were observed at suctions above 600 kPa in the axis-translation method in comparison with the HCT method. This small difference might be

associated with water evaporation from the top of the sample when using the axis-translation method. Moreover, the axis-translation method overestimated the AEV of the specimen by approximately 6% in comparison with the HCT measurements, this deemed to be, in part, due to the discontinuous data points produced by the axis-translation technique. The new oedometer cell enables simultaneous and non-destructive measurement of SWRC using both axis-translation and HCT techniques, along with measurement of specimen's volume change during the course of drying and wetting. These features allow for more accurate determination of water retention characteristics (Pasha et al. 2016), in comparison with other methods of SWRC measurement such as pressure plate.

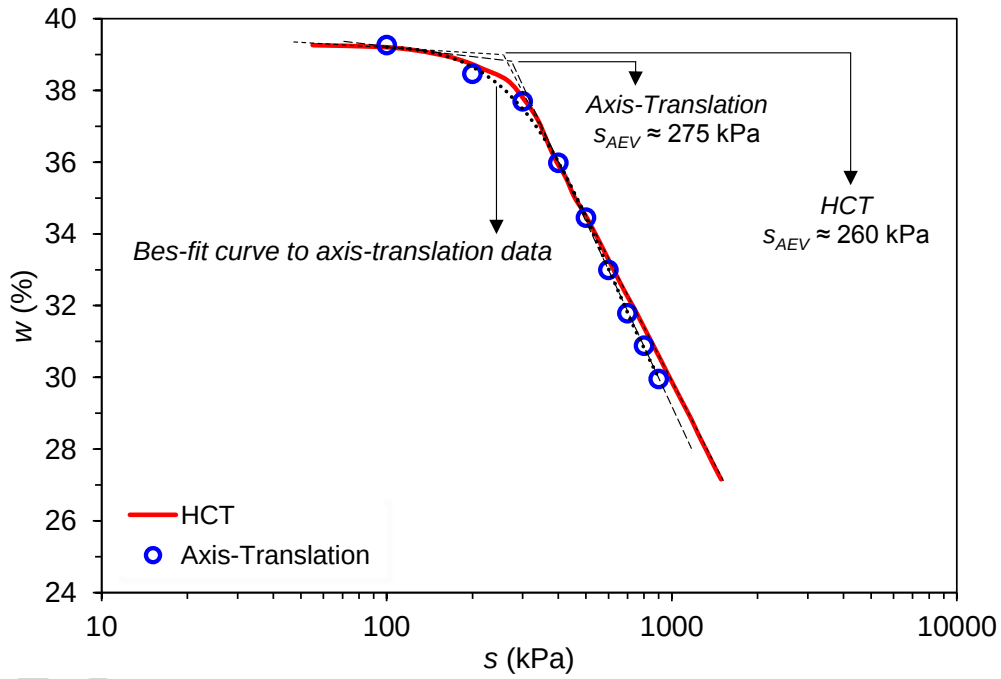

Fig. 8 SWRC determined for main drying path

Figs. 9, 10, and 11 present the results of CRS compression tests performed for evaluating the new oedometer's ability for investigating the coupled effects of strain rate, suction, and temperature. Simplified methods for calculation of unsaturated effective stress can be found in Khoshghalb and Khalili (2013) and Khoshghalb et al. (2015). However, in this work, the mechanical path is represented in terms of axial strain (ε_a) and vertical net stress ($\sigma_v - u_a$). Also

shown in the graphs, are the change in pore-water pressure (Δu) with net stress (dotted lines). For the sake of simplicity, the yield vertical net stress (σ_p) was determined as the intersection of the best fitted lines to the pseudo-elastic and plastic sections of the compression curve.

Inspection of suction evolutions recorded by the HCTs revealed that a suction state was preserved during the compression stages of the carried out experiments, confirming that no water has been expelled from the unsaturated specimens, and hence, the condition of constant water content was recognised. The new cell enables continuous monitoring of stress and strain variations and more accurate estimation of σ_p in comparison with the IL tests. At constant suction, an increase in σ_p was observed with increase in strain rate (Fig. 9). Similarly, at constant strain rate, an increase in suction resulted in an increase in σ_p (Fig. 10). Moreover, at constant suction and strain rate, an increase in temperature resulted in a decrease in σ_p (Fig. 11). Similar results have been reported in the literature. For instance, François et al. (2007) and Salager et al. (2008) performed a set of temperature controlled oedometer tests on unsaturated sandy silt material from the region of Sion in Switzerland, and reported an increase in σ_p with increase in suction, and a decrease in σ_p with increase in temperature. Pereira and De Gennaro (2010) performed isotropic compression tests on unsaturated chalk material at various strain rates and reported an increase in σ_p with increase in strain rate. Similar results (i.e. increase in σ_p with suction and decrease in σ_p with temperature) were reported by Uchaipichat and Khalili (2009) from a set of suction and temperature controlled isotropic tests on a laboratory-compacted silt from the Bourke region of New South Wales, Australia.

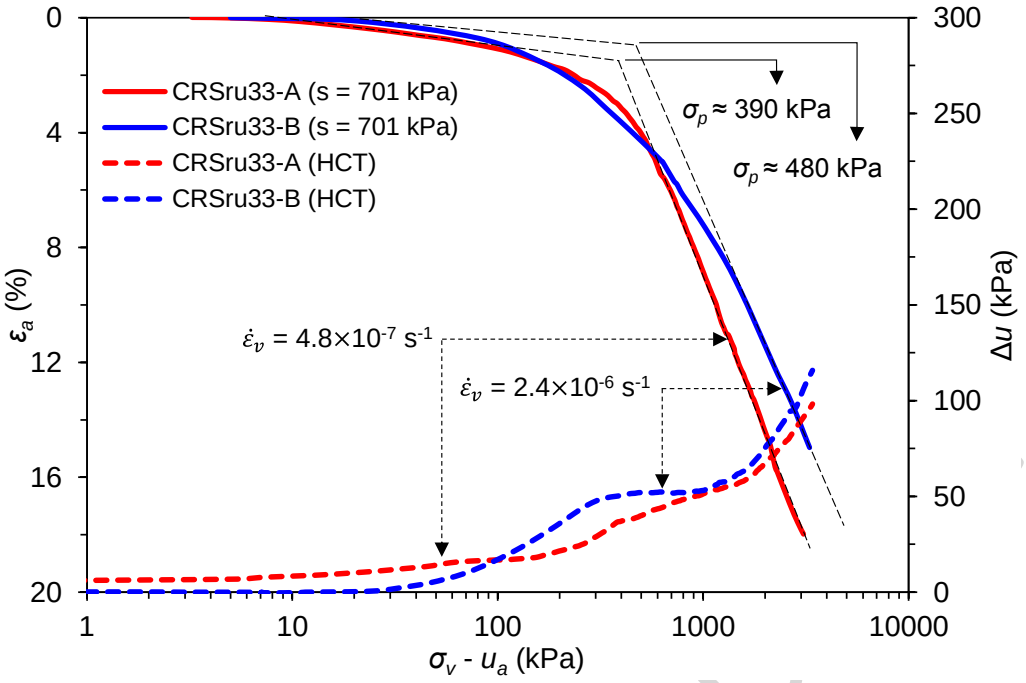

Fig. 9 Effect of strain rate on compression response at constant suction

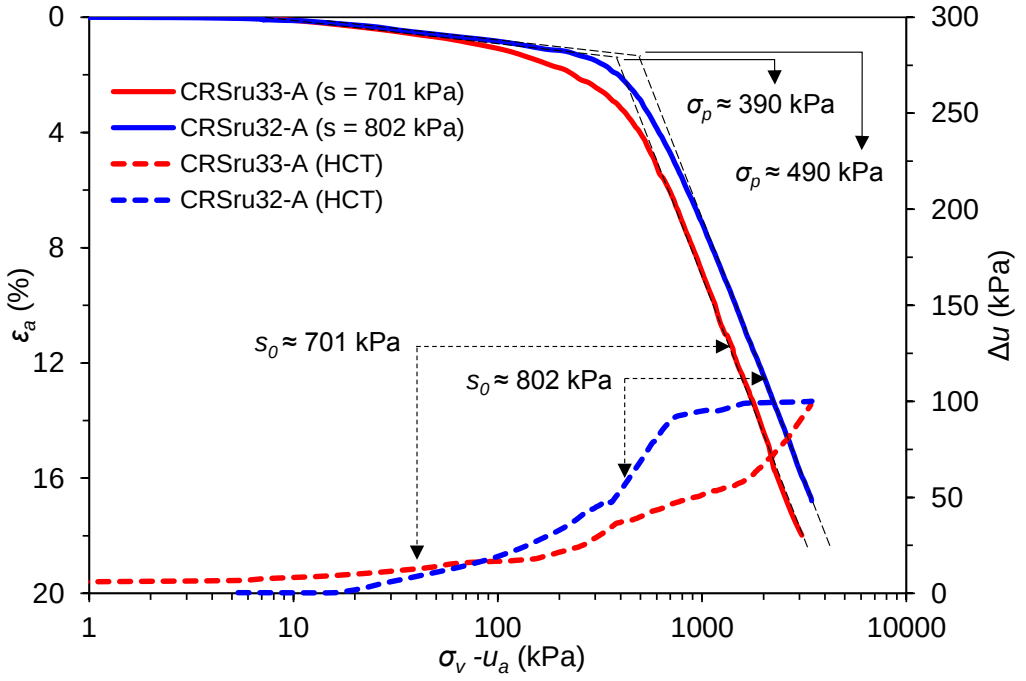

Fig. 10 Effect of suction on compression response at constant strain rate

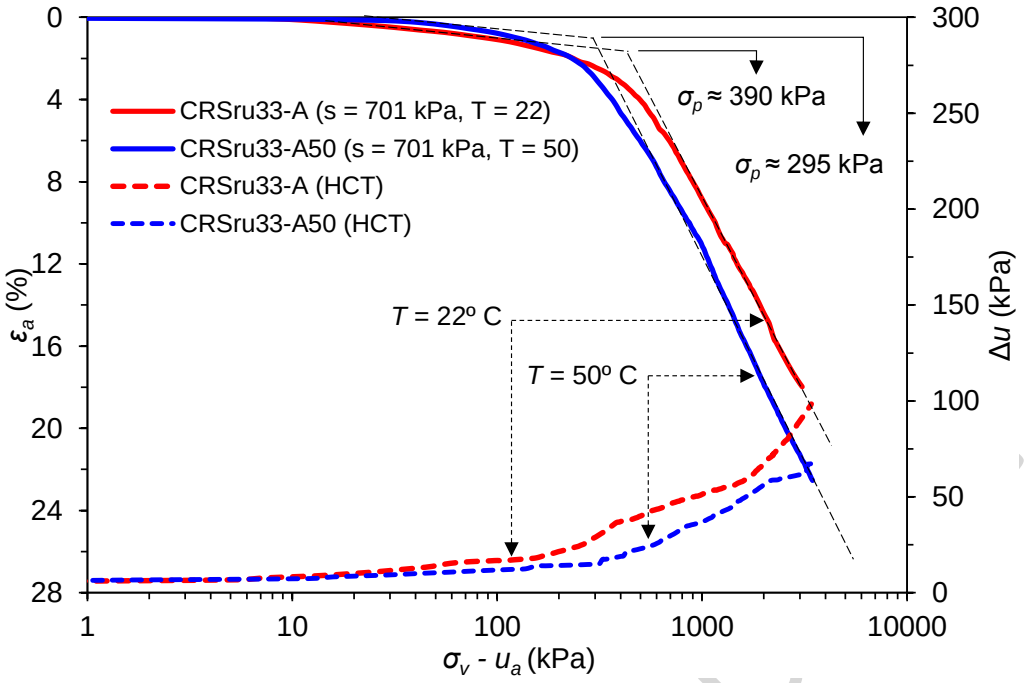

Fig. 11 Effect of temperature on compression response at constant suction and strain rate

In order to investigate the effect of temperature on HCT measurements during an experiment, a soil specimen was subjected to a heating/cooling cycle of 25 to 65º C in steps of 10º C (Fig. 12). For each stage of heating, a sudden increase in u_w (decrease in suction) followed by dissipation of the developed u_{exc} was observed. Similarly, for each stage of cooling, a decrease in u_w (increase in suction) followed by a return of measurements to their initial values was observed. Overall, throughout the course of heating and cooling, a small increase in soil suction was observed. The reason behind the observed increase in soil suction is unknown. The heating cycle may change the structural properties of the localized unsaturated pockets in the specimen in vicinity of the HCTs and hence affect the suction measurements. These possible changes may not be fully recovered during the cooling cycle resulting in less evident suction changes during cooling steps. Fig. 13 shows the axial deformation of the specimen during heating and cooling cycles. The vertical displacements were corrected, for the effect of cell structure dilation, based on the Equation 1. Development and the subsequent dissipation of the u_{exc}

during stepwise heating resulted in development of volumetric strain in the specimen as shown in Fig. 14.

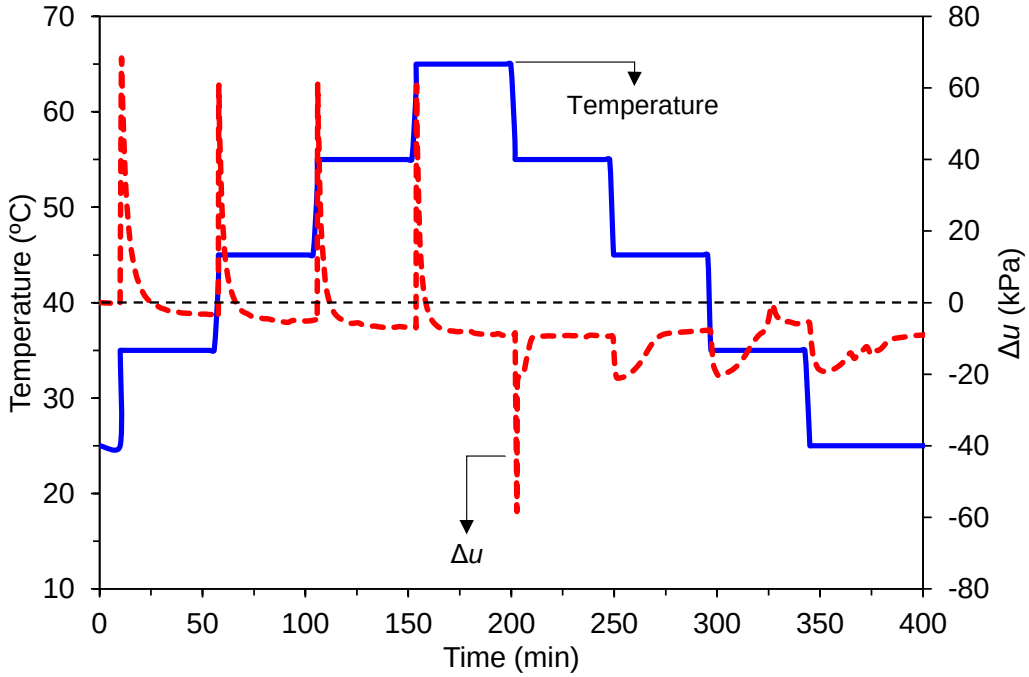

Fig. 12 Effect of temperature on HCT measurement

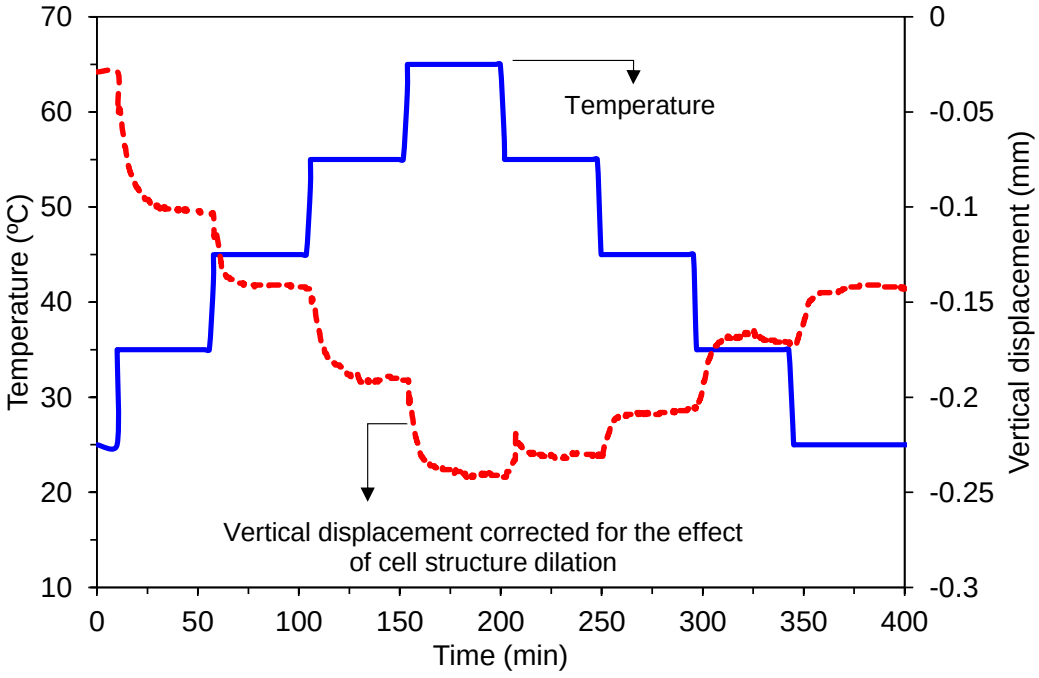

Fig. 13 Vertical displacement of the soil specimen during heating and cooling cycles

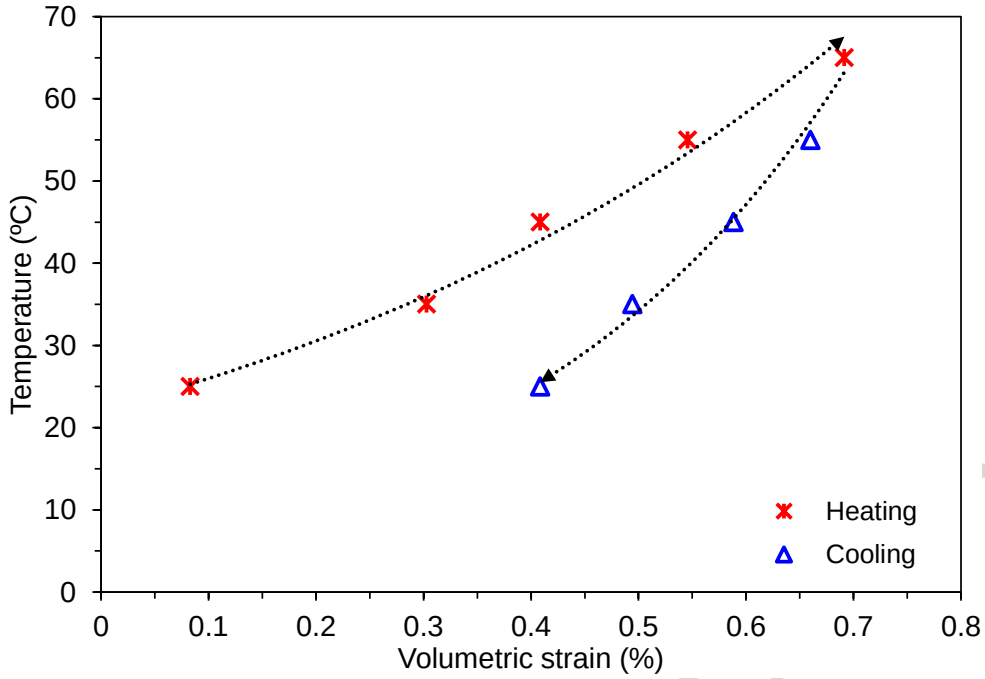

Fig. 14 Thermally induced volumetric strain during heating and cooling cycles

Conclusions

Climatic variations results in development of non-isothermal and unsaturated conditions in soil deposits, arising the need for advanced experimental characterization of soils' mechanical response taking into account the coupled effects of temperature, suction, and loading rate. The specific features of the newly designed cell enables precise investigation of the THM properties of soils over suction, temperature, and strain rate ranges of practical interest. The distinct features of the new cell are

- Incorporation of two suction measurement/control techniques, i.e. axis-translation and HCT, for enhanced and accurate monitoring of suction evolutions especially in long-term tests.
- Enlarged specimen size to capture the macrostructural effects on the THM response of natural clays.
- Broad temperature measurement range of up to 200° C.

- Significant reduction in the equilibrium time by using a tubular heating element at the base of the cell to overcome the delays associated with thermal conductivity of the metallic cell body.

The reliability of the experimental results is a function of adequate calibration of the testing system. The new cell was rigorously calibrated to account for the delay in thermal equilibrium between the heating system and the specimen, and the effect of temperature on cell structure deformation and the response of HCTs. The calibration coefficient of the HCT was found to be unaffected by change in temperature. The paper also presents useful information on necessary corrections to be applied to the measured data using THM cells.

The preliminary results of SWRC measurement and CRS compression tests with this apparatus are promising for its application in soil mechanics laboratories. The results of constant water content tests where temperature, suction, and strain rate were modified, have been presented. It was shown that the cell is capable of measuring and observing the changing trends in the preconsolidation stress with temperature, strain rate, and suction.

Acknowledgments

The authors are grateful to Mr Graeme Thacker of the engineering workshop at the University of Warwick for his useful suggestions in design and manufacturing the apparatus presented.

References

ASTM International. 2006. *Standard Test Method for One-dimensional Consolidation Properties of Saturated Cohesive Soils Using Controlled-strain Loading*. ASTM D4186(2006). West Conshohocken, PA: ASTM International, https://doi.org/10.1520/D4186-06

514 Bagheri, M., M. Rezania and M. Mousavi Nezhad. 2015. "An Experimental Study of the Initial
515 Volumetric Strain Rate Effect on the Creep Behaviour of Reconstituted Clays." *IOP*
516 *Conference Series: Earth and Environmental Science 26*, no. 1: 012034.
517 Bagheri, M., M. Rezania and M. Mousavi Nezhad. 2018. "Cavitation in High-Capacity
518 Tensiometers: Effect of Water Reservoir Surface Roughness." *Geotech Research* 5,
519 no.2: 81-95, https://doi.org/10.1680/jgere.17.00016
520 Burghignoli, A., A. Desideri and S. Miliziano. 2000. "A Laboratory Study on
521 Thermomechanical Behaviour of Clayey Soils." *Can Geotech J* 37, no. 4: 764-780,
522 https://doi.org/10.1139/t00-010
523 Cekerevac, C. and L. Laloui. 2004. "Experimental Study of Thermal Effects on the Mechanical
524 Behaviour of a Clay." *Int J Numer Anal Methods Geomech* 28, no. 3: 209-228,
525 https://doi.org/10.1002/nag.332
526 Coccia, C.J.R. and J.S. McCartney. 2016. "Thermal Volume Change of Poorly Draining Soils
527 I: Critical Assessment of Volume Change Mechanisms." *Comp Geotech* 80
528 (December): 26-40, https://doi.org/10.1016/j.compgeo.2016.06.009
529 Craig, R.F. 2004. *Craig's Soil Mechanics*. London: Spon Press.
530 Delage, P., N. Sultan and Y.J. Cui. 2000. "On the Thermal Consolidation of Boom Clay" *Can*
531 *Geotech J* 37, no. 2: 343-354, https://doi.org/10.1139/t99-105
532 Fodil, A., W. Aloulou and P.Y. Hicher. 1997. "Viscoplastic Behaviour of Soft Clay"
533 *Géotechnique* 47, no. 3: 581-591, https://doi.org/10.1680/geot.1997.47.3.581
534 François, B. and L. Laloui. 2010. "An Oedometer for Studying Combined Effects of
535 Temperature and Suction on Soils." *Geotech Test J* 33, no. 2: 112-122,
536 https://doi.org/10.1520/GTJ102348

François, B., S. Salager, M.S. El Youssoufi, D. Ubals Picanyol, L. Laloui and C. Saix. 2007. "Compression Tests on a Sandy Silt at Different Suction and Temperature Levels." *Comp Appl Geotech Eng GSP* 157: 1-10, https://doi.org/10.1061/40901(220)11

Garga, V.K.. 1988. "Effect of Sample Size on Consolidation of a Fissured Clay." *Can Geotech J* 25, no. 1: 76-84, https://doi.org/10.1139/t88-009

Gasparre, A. "Advanced labortory characterisation of London Clay." PhD diss, University of London, 2005.

Jarad, N., O. Cuisinier and F. Masrouri. 2017. "Effect of Temperature and Strain Rate on the Consolidation Behaviour of Compacted Clayey Soils." *Europ J Environ Civil Eng* 21: 1-18, https://doi.org/10.1080/19648189.2017.1311806

Khoshghalb, A. and N. Khalili. 2013. "A Meshfree Method for Fully Coupled Analysis of Flow and Deformation in Unsaturated Porous Media." *Int J Numeric Anal Methods Geomech* 37, no. 7: 716-743, https://doi.org/10.1002/nag.1120

Khoshghalb, A., A.Y. Pasha and N. Khalili. 2015. "A Fractal Model for Volume Change Dependency of the Water Retention Curve." *Géotechnique* 62, no. 2: 141-146, https://doi.org/10.1680/geot.14.T.016

Lai, X., S. Wang, H. Qin and X. Liu. 2010. "Unsaturated Creep Tests and Empirical Models for Sliding Zone Soils of Qianjiangping Landslide in the Three Gorges." *J Rock Mech Geotech Eng* 2, no. 2: 149-154, https://doi.org/10.3724/SP.J.1235.2010.00149

Le, T. M., B. Fatahi and H. Khabbaz. 2012. "Viscous Behavior of Soft Clay and Inducing Factor." *Geotech Geolog Eng* 30, no. 5: 1069-1083, https://doi.org/10.1007/s10706-012-9535-0

Marinho, F.A.M., W.A. Take and A. Tarantino. 2008. "Measurement of Matric Suction Using Tensiometric and Axis Translation Techniques." *Geotech Geolog Eng* 26, no. 6: 615-631, http://dx.doi.org/10.1007/s10706-008-9201-8

562 Muñoz-castelblanco, J., P. Delage, J.M. Pereira and Y.J. Cui. 2011. "Some Aspects of the
563 Compression and Collapse Behaviour of an Unsaturated Natural Loess." *Géotech*
564 *Letters* 1, no. 2: 17-22, https://doi.org/10.1680/geolett.11.00003
565 Ng, C.W.W. and J. Xu. 2012. "Effects of Current Suction Ratio and Recent Suction History on
566 Small-Strain Behaviour of an Unsaturated Soil." *Can Geotech J* 49, no. 2: 226-243,
567 https://doi.org/10.1139/t11-097
568 Ng, C.W.W, Q.Y. Mu and C. Zhou. 2017. "Effects of Boundary Conditions on Cyclic Thermal
569 Strains of Clay and Sand." *Géotech Letters* 7, no. 1: 1-6,
570 https://doi.org/10.1680/jgele.16.00155
571 Pagano, A., A. Tarantino, M. Bagheri, M. Rezania and Ph. Sentenac. "An Experimental
572 Investigation of the Independent Effect of Suction and Degree of Saturation on Very
573 Small-Strain Stiffness of Unsaturated Sand." Proceedings of Third European
574 Conference on Unsaturated Soils, E-UNSAT2016, September 12–14, 2016, E3S Web
575 of Conferences 9: 1-4, https://doi.org/10.1051/e3sconf/20160914015
576 Pasha A.Y., A. Khoshghalb and N. Khalili. 2016. "Pitfalls in Interpretation of Gravimetric
577 Water Content–Based Soil-Water Characteristic Curve for Deformable Porous Media."
578 *Int J Geomech* 16, no. 6: D4015004, https://doi.org/10.1061/(ASCE)GM.1943-
579 5622.0000570
580 Pereira, J.M. and V. De Gennaro, "On the Time-Dependent Behaviour of Unsaturated
581 Geomaterials." Proceedings of Fifth International Conference on Unsaturated Soils,
582 Barcelona, Spain, September 6–8, 2010, pp. 921-925.
583 Rampino, C., C. Mancuso and F. Vinale. 1999. "Laboratory Testing on an Unsaturated Soil:
584 Equipment, Procedures, and First Experimental Results." *Can Geotech J* 36, no. 1: 1-
585 12, https://doi.org/10.1139/t98-093

586 Rezania, M., M. Bagheri, M. Mousavi Nezhad and N. Sivasithamparam. 2017. "Creep Analysis
587 of an Earth Embankment on Soft Soil Deposit with and without PVD Improvement."
588 *Geotext Geomemb* 45, no. 5: 537-547,
589 https://doi.org/10.1016/j.geotexmem.2017.07.004
590 Rezania, M., M. Mousavi Nezhad, H. Zanganeh, J. Castro and N. Sivasithamparam. 2016.
591 "Modeling Pile Setup in Natural Clay Deposit Considering Soil Anisotropy, Structure,
592 and Creep Effects: Case Study." *Int J Geomech* 17, no. 3: 04016075,
593 https://doi.org/10.1061/(ASCE)GM.1943-5622.0000774
594 Romero, E., A. Gens and A. Lloret. 2003. "Suction Effects on a Compacted Clay under Non-
595 Isothermal Conditions." *Géotechnique* 53, no. 1: 65-81,
596 https://doi.org/10.1680/geot.2003.53.1.65
597 Romero, E., A. Lloret and A. Gens. "Development of a New Suction and Temperature
598 Controlled Oedometer Cell." Proceedings of First International Conference on
599 Unsaturated Soils, Paris, September 6–8, 1995, A.A. Balkema/Presses des Ponts et
600 Chaussees, pp. 553-559.
601 Romero, E., M.V. Villar and A. Lloret. 2005. "Thermo-Hydro-Mechanical Behavior of Two
602 Heavily Overconsolidated Clays." *Eng Geology J* 81, no. 3: 255-268,
603 https://doi.org/10.1016/j.enggeo.2005.06.011
604 Rowe, P.W. and L. Barden. 1966. "A New Consolidation Cell." *Géotechnique* 16, no. 2: 162-
605 170, https://doi.org/10.1680/geot.1966.16.2.162
606 Salager, S., B. François, M.S. El Youssoufi, L. Laloui and C. Saix. 2008. "Experimental
607 Investigations on Temperature and Suction Effects on Compressibility and Pre-
608 Consolidation Pressure of a Sandy Silt." *Soils Found* 48, no. 4: 453–466,
609 https://doi.org/10.3208/sandf.48.453

610 Sample, K.M. and C.D. Shakelford. 2012. "Apparatus for Constant Rate-of-Strain
611 Consolidation of Slurry Mixed Soils." *Geotech Test J* 35, no. 3: 409-419,
612 https://doi.org/10.1520/GTJ103787

613 Seah, T.H. and T. Juirnarongrit. 2003. "Constant Rate of Strain Consolidation with Radial
614 Drainage." *Geotech Test J* 26, no. 4: 432-443, https://doi.org/10.1520/GTJ11251J

615 Tarantino, A. and E. De Col. 2008. "Compaction Behavior of Clay." *Géotecnique* 58, no. 3:
616 199-213, https://doi.org/10.1680/geot.2008.58.3.199

617 Tsutsumi, A. and H. Tanaka. 2011. "Compressive Behavior During the Transition of Strain
618 Rate." *Soils Found* 51, no. 5: 813-822, https://doi.org/10.3208/sandf.51.813

619 Uchaipichat, A. and N. Khalili. 2009. "Experimental Investigation of Thermo-Hydro-
620 Mechanical Behaviour of an Unsaturated Silt." *Géotecnique* 59, no. 4: 339-353,
621 https://doi.org/10.1680/geot.2009.59.4.339

622 Wissa, A.E.Z. and S. Heiberg, "A New One-Dimensional Consolidation Test," Department of
623 Civil Engineering Research Report 69-9, Soil Publication, No. 229, Massachusetts
624 Institute of Technology, Cambridge, MA, 1969.

625 Zou, L., S. Wang and X. Lai. 2013. "Creep Model for Unsaturated Soils in Sliding Zone of
626 Qianjiangping Landslide." *J Rock Mech Geotech Eng* 5, no. 2: 162-167,
627 https://doi.org/10.1016/j.jrmge.2013.03.001.